

Processing X/K band radio occultation data in the presence of turbulence

M. E. Gorbunov

Obukhov Institute for Atmospheric Physics, Moscow, Russia

Institute for Geophysics, Astrophysics, and Meteorology, University of Graz, Graz, Austria

G. Kirchengast

Institute for Geophysics, Astrophysics, and Meteorology and Wegener Center for Climate and Global Change, University of Graz, Graz, Austria

Received 2 March 2005; revised 27 July 2005; accepted 10 August 2005; published 15 November 2005.

[1] Canonical transform (CT) and full-spectrum inversion (FSI) methods can be used in processing radio occultation data to retrieve transmission profiles, which are necessary in addition to bending angle profiles for the retrieval of atmospheric humidity independent of temperature. Low Earth orbiter–low Earth orbiter cross-link occultations with X/K band frequencies can provide transmission data along the wing of the 22 GHz water vapor absorption line. The computation of transmission assumes spherical symmetry of the atmospheric real and imaginary refractivity. This condition is broken in the presence of turbulence, which can result in significant errors in transmission. We suggest the computation of the differential transmission from the differential CT/FSI amplitude to correct for the effect of turbulence. The efficiency of the method is tested by quasi-realistic numerical end-to-end simulations. We explicitly modeled turbulence as random refractivity fluctuation field based on power form of the fluctuation spectrum. The simulations demonstrate that the error in the retrieved transmission can be significant in a single frequency channel, while the differential transmission can be retrieved with high accuracy. The new method does not impose any significant restriction on the frequency difference between the channels and provides very good differential transmission sensitivity if spacings of a few gigahertz are chosen (e.g., 10 and 17 GHz or 17 and 20 GHz).

Citation: Gorbunov, M. E., and G. Kirchengast (2005), Processing X/K band radio occultation data in the presence of turbulence, *Radio Sci.*, 40, RS6001, doi:10.1029/2005RS003263.

1. Introduction

[2] Radio occultations using GPS signals proved to be a very powerful technique for sounding the Earth's atmosphere [Kursinski *et al.*, 2000]. At GPS frequencies there is a noticeable attenuation reaching 1 dB, caused by the diatomic molecules of nitrogen and oxygen. This attenuation is not useful for retrieving water vapor, however, because a retrieval would rely on a cancellation between two very noisy quantities. This makes it impossible to separate the dry and wet terms of the retrieved refractivity without employing additional a priori information. Use of an observation system of low

Earth orbiters (LEOs) implemented with transmitters and receivers of radio signals in the 9–30 GHz band can solve this problem [Yakovlev *et al.*, 1995; Sokolovskiy, 2001; Kursinski *et al.*, 2002; Lohmann *et al.*, 2003b; Kirchengast and Heg, 2004; Kirchengast *et al.*, 2004a, 2004b]. Water vapor has an absorption line centered near 22 GHz. Therefore, from measurements of phase and amplitude, the complex refractive index can be retrieved. Then, pressure, temperature, and water vapor profiles can be solved for, using a spectroscopic model of the water vapor line, the refractivity equation, the hydrostatic equation, and the equation of state. Kirchengast *et al.* [2004b] describe this retrieval processing in detail, but their description is restricted to the geometric-optics approach for the transmission and bending angle retrieval.

[3] Here the focus is on transmission and bending angle retrieval by wave-optical methods, which will be the approach generally required with real data, since the retrieval scheme will encounter a significant challenge in case of diffraction and multipath caused by turbulence. In the lower troposphere, amplitude scintillation may often be strong [Kan *et al.*, 2002; Yakovlev *et al.*, 1995, 2003]. Under these conditions, the amplitude of a radio occultation signal is significantly more sensitive to small-scale turbulence than the phase [Yakovlev *et al.*, 1995; Sokolovskiy, 2001]. In presence of turbulence, the amplitude of the wave field undergoes strong scintillations, which can overwhelm the effect of absorption. In order to reduce the effect of scintillations, it was suggested to use twin frequencies [Gorbunov, 2002a; Gorbunov and Lauritsen, 2002, 2004; Gorbunov *et al.*, 2004; Kursinski *et al.*, 2002; Facheris and Cuccoli, 2003].

[4] Given the measurements of the wave field $u_1(t)$ and $u_2(t)$ for two frequencies f_1 and f_2 , the difference $\Delta f = f_1 - f_2$ being small enough, we consider the ratio of the amplitudes $|u_1(t)/u_2(t)|$. Because for neighboring frequencies the effects of diffraction and interference will not differ significantly, it is expected that they will be reduced in the ratio. The amplitude of the wave field $|u_{1,2}(t)|$ is proportional to the transmission $\exp(-\tau_{1,2})$, where $\tau_{1,2}$ is the integral absorption along a ray: $\tau_{1,2} = k_{1,2} \int n''_{1,2} ds$, and $n''_{1,2}$ is the imaginary part of the refractivity for the frequencies $f_{1,2}$ and corresponding wave numbers $k_{1,2} = 2\pi f_{1,2}/c$. In this case $\ln(u_1(t)/u_2(t))$ equals differential absorption, $\tau_2 - \tau_1$. However, this is only valid if Δf is small enough. On the other hand, choice of too small Δf will result in too low values of the differential absorption, which will increase the noise sensitivity.

[5] The wave optics processing methods such as canonical transform (CT) [Gorbunov, 2002b; Gorbunov and Lauritsen, 2002, 2004; Gorbunov *et al.*, 2004] or full-spectrum inversion (FSI) [Jensen *et al.*, 2003, 2004] transform the wave field into the representation of impact parameter. In this representation, the amplitude describes the distribution of the energy with respect to impact parameters. For a spherically symmetric atmosphere, the amplitude of the transformed wave field is proportional to the exponential function of the integral absorption along the ray, that is, the transmission. Therefore CT and FSI techniques can be used for the retrieval of atmospheric transmission profiles [Gorbunov, 2002b; Jensen *et al.*, 2004]. These techniques will significantly reduce retrieval errors due to multipath and diffraction. However, the problem of turbulence still persists. Because turbulence is a three-dimensional (3-D) inhomogeneous structure, the amplitude of the transformed wave field also indicates scintillations [Sokolovskiy, 2001].

[6] In this study, we suggest the differential method for retrieval of transmission in combination with the CT or

FSI techniques. These methods define the transformed wave field $\hat{\Phi}u_{1,2}(p)$, which, at each single frequency, is to a significant extent free from the effects of diffraction and multipath. These effects may only be significant for atmospheric inhomogeneities with scales below 50 m [Gorbunov *et al.*, 2004]. The logarithmic ratio of the transformed amplitudes $\ln |\hat{\Phi}u_1(p)/\hat{\Phi}u_2(p)|$ will then further suppress the scintillations due to small-scale turbulence and will be equal to the differential absorption $\tau_2 - \tau_1$ with a much higher accuracy than the direct amplitude ratio $\ln (|u_1(t)/u_2(t)|)$.

[7] We tested the performance of this new type of the differential method in numerical simulations. In the simulations we used 3-D global fields from a European Centre for Medium-Range Weather Forecasts (ECMWF) analysis with superposition of random 2-D turbulence. The simulations include modeling realistic receiver noise assuming a carrier-to-noise density ratio of 67 dBHz (decibels times Hertz), which is the baseline value of LEO-LEO occultation mission ACE+ [Kirchengast and Høeg, 2004].

2. Description of Method

[8] In the framework of the CT method, the retrieval of absorption from the measurements of the complex wave field during a radio occultation experiment, $u(t)$, is performed by the following algorithm. The wave field is transformed to the representation of the impact parameter by the following Fourier integral operator (FIO):

$$\hat{\Phi}u = \sqrt{\frac{-ik}{2\pi}} \int a(p, Y) \exp(ikS(p, Y))u(Y(t))dY, \quad (1)$$

where $k = \frac{2\pi}{\lambda}$ is the wave number, $a(p, Y)$ and $S(p, Y)$ are the amplitude and phase function of the FIO, respectively, and $Y(t)$ is a coordinate along the observation trajectory, which generalizes the use of the angular distance between the satellites θ in the FSI method [Gorbunov and Lauritsen, 2002, 2004; Jensen *et al.*, 2003, 2004]. The amplitude function has the following form [Gorbunov and Lauritsen, 2004]:

$$a(p, Y) = \left(\sqrt{r_R^2 - p^2} \sqrt{r_T^2 - p^2} \frac{r_R r_T}{p} \sin \theta \right)^{1/2}, \quad (2)$$

where r_T and r_R are (LEO) transmitter and (LEO) receiver satellite radii. Here r_T , r_R , and θ are derived from the satellite orbit data and are represented as functions of time t or the new orbit parameter $Y(t)$. The transmission profiles $\tau_{1,2}(p)$ are retrieved from the amplitudes of the transformed wave field using the relationship $A_{1,2}(p) \equiv |\hat{\Phi}u_{1,2}| = A_{1,2} \exp(-\tau_{1,2}(p))$, where $A_{1,2}$ are normalizing constants [Gorbunov, 2002b]. These equations for the

amplitude function and transmission retrieval assume the spherical symmetry.

[9] In order to evaluate the influence of the horizontal gradients, the asymptotic solution for the forward simulation of the wave field can be expressed in terms of the inverse FIO with the following amplitude function [Gorbunov and Lauritsen, 2004]:

$$a^*(Y, p) = \left(\frac{1}{\sqrt{r_R^2 - p_R^2} \sqrt{r_T^2 - p_T^2}} \frac{p_T}{r_R r_T \sin \theta} \frac{dp_T}{dp} \right)^{1/2}, \quad (3)$$

where p_T and p_R are the impact parameters at transmitter and receiver satellite, and p is the effective impact parameter computed from the Doppler frequency shift by way of the classical geometric-optical bending angle retrieval.

[10] For a spherically symmetric atmosphere, $p_R = p_T = p$. Generally, because of horizontal gradients, these three impact parameters are different, and the following equation can be established [Gorbunov and Kornblueh, 2001]:

$$p_R = p_T + \int \frac{\partial n}{\partial \theta} ds, \quad (4)$$

where the integral is taken along the ray. Here p_R and p_T can be expressed as functions of the effective impact parameter p . The relation between p , p_R , and p_T includes the horizontal gradient of refractive index $\frac{\partial n}{\partial \theta}$, which is unknown a priori.

[11] The amplitude of the transformed wave field retrieved by the CT or FSI method is found to equal the following expression:

$$A_{1,2}(p) = \bar{A}_{1,2} \frac{\sqrt{r_R^2 - p^2} \sqrt{r_T^2 - p^2}}{\sqrt{r_R^2 - p_R^2} \sqrt{r_T^2 - p_T^2}} \frac{p_T}{p} \frac{dp_T}{dp} \cdot \exp(-\tau_{1,2}(p)) \equiv \bar{A}_{1,2} K(p) \exp(-\tau_{1,2}(p)). \quad (5)$$

This expression is represented as a composition of the normalizing constant $\bar{A}_{1,2}$, transmission along the ray $\exp(-\tau_{1,2}(p))$, and the corrupting term $K(p)$ that depends on the horizontal gradients. For a spherically layered medium, factor $K(p)$ equals unity, and transmission can be retrieved from the CT or FSI amplitude. For a 3-D medium with horizontal gradients, factor $K(p)$ approximately equals $\frac{dp_T}{dp}$, which differs from unity. This shows that in the presence of 3-D inhomogeneities, in particular, atmospheric turbulence, the amplitude of the transformed wave field $A_{1,2}(p)$ will undergo scintillations. Because factor $K(p)$ is not independently retrievable from observables and therefore is unknown a

priori, the error of the retrieved logarithmic transmission $\tau_{1,2}(p)$ in each channel will be of size $\ln K(p)$.

[12] It is important to recognize that $K(p)$ does not depend on the frequency of the wave field. The dependence of measured wave field $u_{1,2}(t)$ upon frequency is involved through diffraction and interferences due to multipath. The FIO introduced in the CT method includes the inversion of the wave front (back propagation) and eliminates multipath propagation and diffraction effects due to the long-distance propagation from the planet limb to the space-borne receiver [Gorbunov, 2002a; Gorbunov et al., 2004; Gorbunov and Lauritsen, 2004]. As discussed by Gorbunov et al. [2004], this operator does not correct for effects of diffraction on small-scale inhomogeneities inside the atmosphere.

[13] Therefore the term $\ln K(p)$ will cancel in the differential transmission $\tau_2(p) - \tau_1(p)$, and only some residual diffractive effects will be left. These residual errors are best assessed by numerical simulations as discussed below. The normalizing constants $\bar{A}_{1,2}$ are estimated from the wave field at heights 25–30 km. The logarithmic ratio of the normalized amplitudes can be expressed as follows:

$$\ln \frac{A_1(p)/\bar{A}_1}{A_2(p)/\bar{A}_2} = \tau_2(p) - \tau_1(p). \quad (6)$$

Here logarithmic transmissions $\tau_{1,2}(p)$ are measured in Neper. Multiplication with a factor of $(20/\ln 10)$ will convert them to decibels.

[14] The described method is assessed and verified below by rigorous wave optical forward-inverse simulations with fields containing severe small-scale random turbulence and thermal receiver noise.

3. Numerical Simulation Results

[15] A quasi-realistic model of the turbulent atmosphere was adopted, which includes a regular part from ECMWF analyses complemented with anisotropic turbulence with a magnitude chosen according to radiosonde measurements. Turbulence was modeled as a random relative perturbation of the refractivity field with a power form of the spectrum:

$$\tilde{B}(\kappa) = \begin{cases} \tilde{C} \kappa^{-\mu}, & \kappa < \kappa_{ext} \\ \tilde{C} \kappa^{-\mu}, & \kappa_{ext} \leq \kappa \leq \kappa_{int} \\ \tilde{C} \kappa^{-\mu} \exp \left[- \left(\frac{\kappa - \kappa_{int}}{\kappa_{int}/4} \right)^2 \right], & \kappa > \kappa_{int}, \end{cases} \quad (7)$$

where $\kappa = (\kappa_z^2 + q^2 \frac{\kappa_\theta^2}{r^2})^{1/2}$, κ_z and κ_θ are the spatial frequencies (wave numbers) conjugated to the polar coordinates z ; θ in the occultation plane (z being the

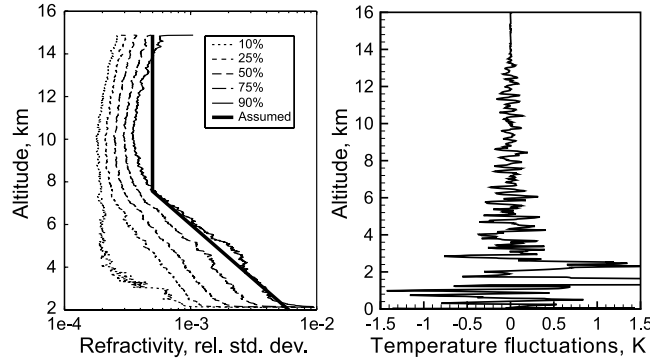


Figure 1. (left) Estimation of RMS profiles of turbulent fluctuations on the basis of a data set of high-resolution radiosonde observation profiles observed at St. Helena (“low latitude”: 15.6°S, 5.4°W): median profile (50%) and different percentiles. The profile “Assumed” (thick black line), meant to roughly reflect the upper decile (90%), is the one used for the turbulence modeling in this study. (Figure adapted courtesy of S. Buehler, University of Bremen, Bremen, Germany). (right) Turbulent fluctuations of the retrieved dry temperature.

height above the Earth’s surface, θ being the polar angle); and q is the anisotropy coefficient ($q > 1$, horizontally stretched turbulence), and r_E is the Earth’s radius. The factor \tilde{c} normalizes the RMS turbulent fluctuations to unity. In the coordinate space we use an additional factor $c(z)$, which describes the relative magnitude of turbulent perturbations as a function of altitude.

[16] We selected a tropical occultation case with severe turbulence, that is, an extreme case affecting <10% of globally observed X/K band occultations, while >90% of occultations are expected to experience more favorable conditions. Figures 1 and 2 illustrate the atmospheric conditions for this case. Figures 2, 3, and 4 show the results of the simulation. The turbulence is characterized by external scale $2\pi/\kappa_{ext} = 0.1$ km, internal scale $2\pi/\kappa_{int} = 0.03$ km, exponent $\mu = 4$ for the 2-D spectrum (corresponding to exponent $\mu_{3D} = 5$ for the 3D spectrum), and anisotropy $q = 10$. Using standard formulas [Tatarskii, 1961], we can derive the corresponding structure function $D(r) \propto r^{\mu_{3D}-3} = r^{\mu-2} = r^2$, where $r = (\Delta z^2 + (r_E \frac{\Delta\theta}{q})^2)^{1/2}$, provided that Δz and $r_E \frac{\Delta\theta}{q}$ are confined between the internal and external scales.

[17] As shown by Gurvich [1984, 1989] and Gurvich and Brekhovskikh [2001], an increase in anisotropy does not significantly change the turbulent fluctuation of refraction angles. This is also corroborated by another simulation with $q = 20$ (not shown here [see Gorbunov and Kirchengast, 2005]), which indicates perhaps slightly enhanced bending angle and transmission errors, but the difference compared to $q = 10$ is very small. The magnitude $c(z)$ was set according to the refractivity fluctuation climatology from high-resolution low-latitude radiosonde observations on St. Helena Island (S. Buehler,

University of Bremen, private communication, 2004): $c(z)$ equals 0.006 at a height of 2.0 km and logarithmically decreases to 0.0005 at a height of 7.5 km. This corresponds to effective temperature variations of 1.5 K at a height of 2.0 km and 0.15 K at a height of 7.5 km. Outside this interval, $c(z)$ is assumed to be constant with height.

[18] This model and the parameters chosen provide a realistic spectrum for the free atmosphere (above the atmospheric boundary layer) according to theoretical and experimental studies [Gurvich and Chunchuzov, 2003, 2005; Fritts et al., 1988; Fritts and VanZandt, 1993; Fritts and Alexander, 2003; Gurvich and Brekhovskikh, 2001; Gurvich and Chunchuzov, 2003, 2005]. The experimental studies [Gurvich and Chunchuzov, 2003, 2005] based on stellar occultations revealed that the atmospheric turbulence can be represented as a superposition of isotropic component (Kolmogorov turbulence with $\mu_{3D} = 11/3$) and anisotropic component with $\mu_{3D} = -5$. The anisotropic component has a spectrum close to that of internal gravity waves. Our model adopts the spectrum of anisotropic refractivity fluctuations discussed by Gurvich and Chunchuzov [2003, 2005]. A close value of $\mu_{3D} = 4.5$ was obtained by Yakovlev et al. [2003].

[19] We adopted an internal scale of 30 m, which exceeds the typical values of 1–10 m found by Gurvich and Chunchuzov [2003]. According to Yakovlev et al. [2003] and Kan et al. [2002], the amplitude scintillation spectra for a wavelength of 2 cm (15 GHz) at scintillation frequencies >20 Hz provide a very small contribution into the scintillation power, due to the steep spectral slope. For the characteristic vertical scan velocity of 1 km/s in the troposphere, this frequency range with small contribution corresponds to inhomogeneities with

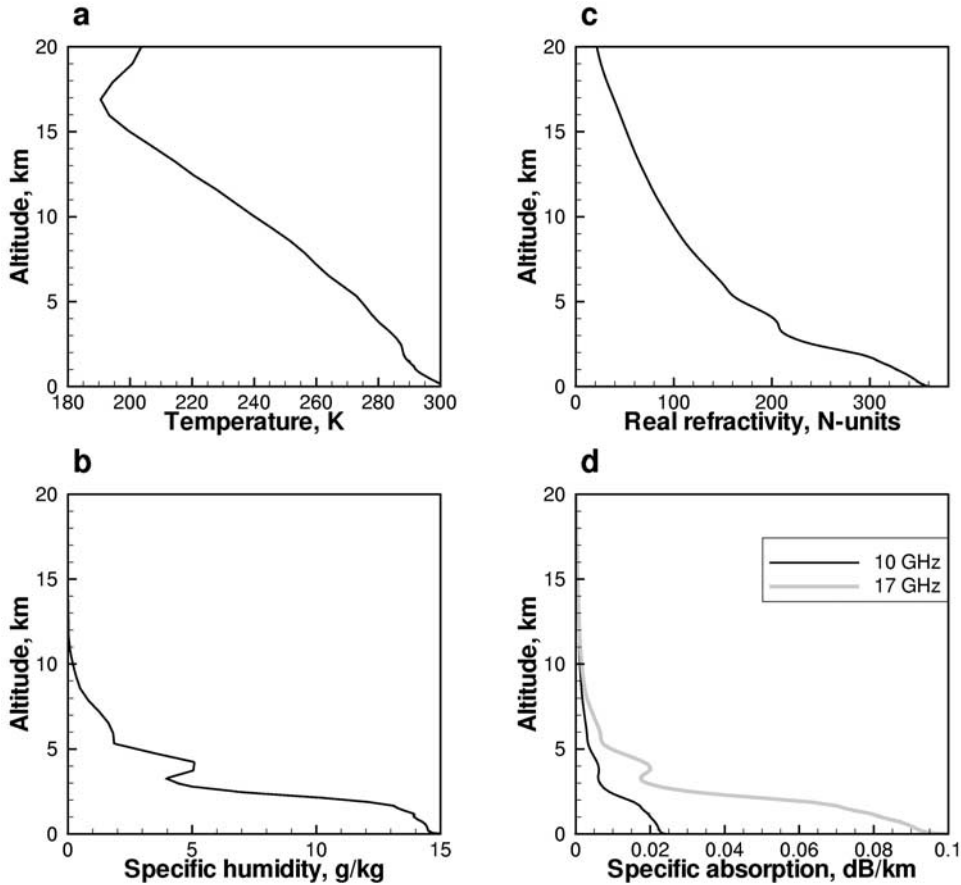


Figure 2. Simulated occultation event 0118 (29 May 2001; 1312 UTC; 10.4°S, 140.7°E; ECMWF field with superimposed power turbulence; frequency channels 10 and 17 GHz): (a) temperature, T , for the regular medium and dry temperature, $T_{\text{dry}}^{(\text{turb})}$, for the turbulent medium; (b) specific humidity, q ; (c) real refractivity, N ; and (d) specific absorptions, $(20/\ln 10)kN$, for the two frequencies.

vertical scales <50 m. From a complementary perspective, the modeled internal scale of 30 m approximately corresponds to the diffraction limit derived by *Gorbunov et al.* [2004]: $h \geq \sqrt[3]{2\lambda^2 r_E}$. This is the estimate of the smallest vertical scale of inhomogeneities, which play a significant role in diffraction/scintillation effects; that is, inhomogeneities with smaller scales produce a very small input into amplitude scintillations. A detailed theoretical analysis of this behavior was given by *Tatarskii* [1961], *Ishimaru* [1978], and *Rytov et al.* [1989], who analyzed the input of different spatial frequencies of turbulence into amplitude scintillations and showed that amplitude scintillation frequency is limited at the high-frequency end by diffraction effects.

[20] For the ACE+ case with channels near 15 GHz, the diffractive limit is about 20 m. In the present study we have chosen 30 m in our numerical simulations, as

close as possible to this limit; the difficulties and computational demand for numerical simulations of turbulence in an explicit random field modeling approach increase dramatically with modeling smaller vertical scales. However, while we do not expect significant changes in the results, we might attempt simulations with scales down to 10 m based on further modeling developments, and even faster computers, in the future.

[21] Regarding the choice of anisotropic turbulence, it was shown by *Kan et al.* [2002], *Gurvich* [1984, 1989], and *Gurvich and Brekhovskikh* [2001] that the main input into scintillation above the atmospheric boundary layer (>2 km) comes from anisotropic turbulence. For example, *Gurvich and Brekhovskikh* [2001] analyzed the dependence of the scintillation amplitude on the anisotropy coefficient q and found, backed by experimental

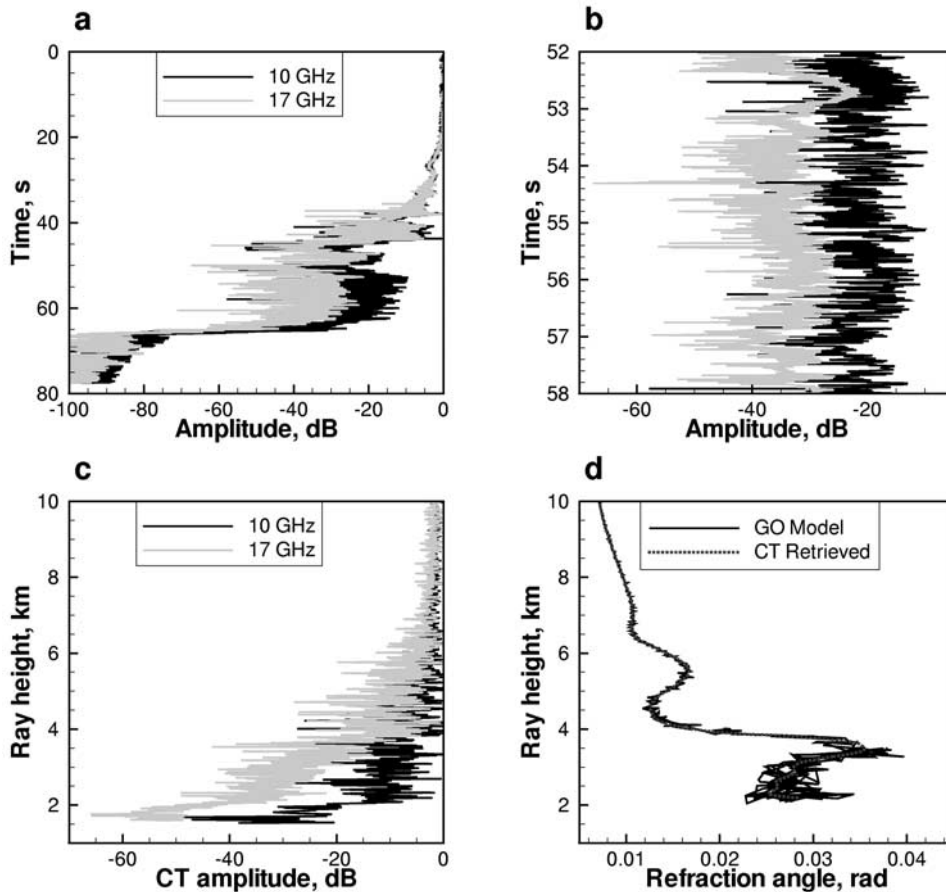


Figure 3. Simulated occultation event 0118 (29 May 2001; 1312 UTC; 10.4°S, 140.7°E; ECMWF field with superimposed power turbulence; frequency channels 10 and 17 GHz): (a) amplitudes in the two channels, (b) enlarged fragment of amplitude records in multipath area, (c) CT amplitudes for the two channels, and (d) refraction angles, simulated using the GO model and retrieved using the CT method.

data, that scintillations increase as q increases from 1 to about 10, then the effect is saturated. The reason is that isotropic turbulence of a given vertical scale has, compared to an anisotropic one, smaller correlation radius horizontally along ray, while the observed along-ray integrated scintillation effect is smaller.

[22] Figure 1 (left) shows the standard deviation of the relative fluctuations of refractive index $\Delta N/N$ obtained from a tropical radiosonde. Figure 1 (right) shows the associated effective temperature fluctuations defined as the difference between the dry temperature profiles computed for the unperturbed atmospheric model without turbulence and for the atmospheric models with turbulence. Figure 2 shows the moist, tropical atmospheric conditions prevailing in the given case.

[23] Simulated amplitudes depicted in Figures 3a and 3b indicate strong turbulent scintillations. We evaluated

the log-amplitude scintillations $\langle |u_{1,2}(t)| - \langle |u_{1,2}(t)| \rangle \rangle / \langle |u_{1,2}(t)| \rangle$, where the angle brackets denote averaging over the time intervals corresponding to a vertical scale of 1.5 km. The log-amplitude scintillations exceed 0.5 below 7 km. The wave field was sampled at 1 kHz. For the application of wave optics processing techniques, it is important that the sampling rate should be high enough to accurately reproduce the interference pattern. In particular, the numerical simulations of absorption retrieval described by *Lohmann et al.* [2003a] indicate large errors in multipath area due to an insufficient sampling rate (about 200 Hz). Figure 3c shows the CT amplitudes computed for both channels. The CT amplitudes also undergo strong scintillations. The effect of turbulence is also visible in the bending angle profiles shown in Figure 3d. The geometric optical (GO) bending angle was computed by means of the forward simulation on

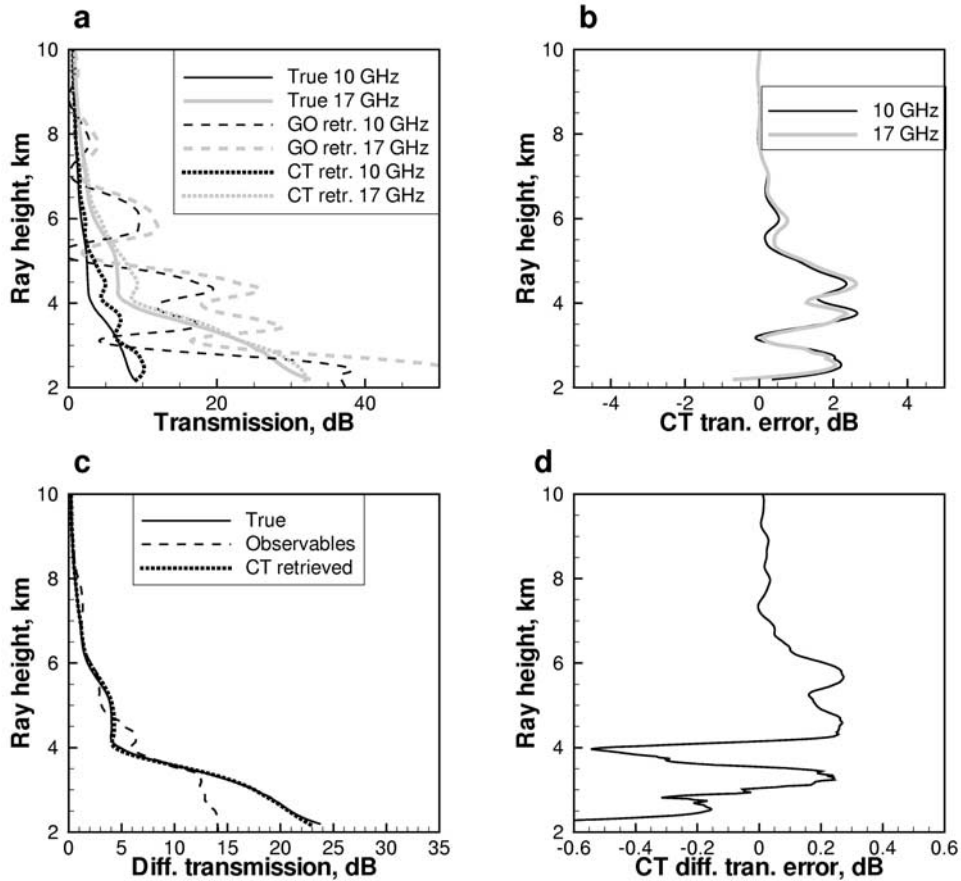


Figure 4. Simulated occultation event 0118 (29 May 2001; 1312 UTC; 10.4°S, 140.7°E; ECMWF field with superimposed power turbulence; frequency channels 10 and 17 GHz): (a) transmissions for the two channels: simulated true, retrieved from the measured amplitudes by GO algorithm, and retrieved from the CT amplitudes; (b) errors of the CT transmission; (c) differential transmission: simulated true, retrieved from the measured amplitudes (observables), and retrieved from the CT amplitudes; and (d) errors of the CT differential transmission.

the basis of ray tracing. The GO bending angle profile indicates small-scale structures due to turbulence. Because turbulent perturbations are not spherically symmetrical, it also results in the random perturbation of the impact parameters. This explains the GO bending angle profile being a multivalued function. The CT algorithm allows for a good retrieval of a smoothed bending angle profile.

[24] Figure 4 shows the result of the retrieval of transmission when disregarding receiver noise. Figure 4a presents the simulated true transmissions for both channels and the retrieved ones. We plot logarithmic transmissions measured in decibels, which equal $(20/\ln 10)\tau_{1,2}(p)$. The retrieval was performed using two different algorithms: (1) the measured amplitude using single-ray geometric optical (GO) approximation, with-

out CT, and (2) the CT amplitude. The GO algorithm defines the transmission as the logarithmic ratio of the measured amplitude and the spreading/defocusing amplitude evaluated from the Doppler frequency shift and satellite orbit data [Kirchengast *et al.*, 2004b]. The plot shows that the CT transmission retrieval provides a much better accuracy than the GO retrieval. Figure 4b shows the CT transmission errors. The errors reach 2 dB below 5 km ray height. However, the transmission errors in the two channels are well correlated. Figure 4c shows the retrieval of the differential transmission. The CT differential transmission is retrieved significantly better compared to the one directly retrieved from the measured amplitudes. Figure 4d shows the CT transmission errors. The correlation of transmission errors in the two channels allows for a significant reduction of the differential

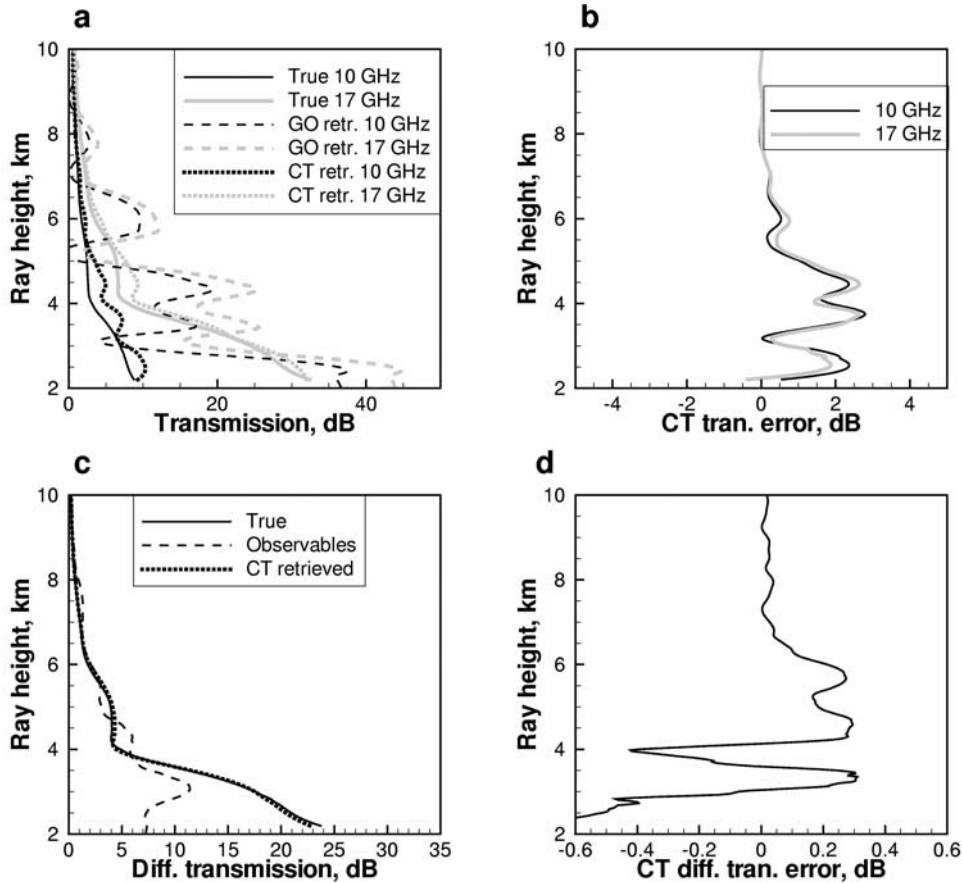


Figure 5. Simulated occultation event 0118 (29 May 2001; 1312 UTC; 10.4°S, 140.7°E; ECMWF field with superimposed power turbulence; frequency channels 10 and 17 GHz) with a model of receiver noise 67 dBHz: (a) transmissions for the two channels: simulated true, retrieved from the measured amplitudes by GO algorithm, and retrieved from the CT amplitudes; (b) errors of the CT transmission; (c) differential transmission: simulated true, retrieved from the measured amplitudes (observables), and retrieved from the CT amplitudes; and (d) errors of the CT differential transmission.

transmission error. Below 6 km, the RMS CT transmission error is 0.28 dB.

[25] Figure 5 shows the results of processing the same simulated event with superimposed receiver noise with a density of 67 dBHz, in line with the ACE+ noise specification. The increase of transmission retrieval errors due to the noise is most visible in the GO retrieval below a ray height of about 3.5 km (approximately 2 km altitude, top of boundary layer), in the area of strong multipath propagation, where the amplitude is low. To reduce the noise influence, we used a radio holographic noise filtering algorithm (M. E. Gorbunov and K. B. Lauritsen, Radio holographic filtering, error estimation, and quality control of radio occultation data, submitted to *Journal of Geophysical*

Research, 2005). In the CT retrieval the noise influence is small. Below 6 km, the RMS CT transmission error is 0.33 dB.

[26] In summary, the CT differential transmission retrieval is found to be accurate throughout the troposphere down to the top of the boundary layer. Gorbunov and Kirchengast [2005], who analyzed more cases, including high-latitude ones, and used different anisotropy settings, found this favorable performance holding for all cases.

4. Discussion of Potential Restrictions

[27] In the numerical simulations we assumed that the real part of the atmospheric refractivity is non-

dispersive. Being rigorous, the real refractivity is not perfectly nondispersive over several GHz spacing: (1) There is the small influence of the 22 GHz water vapor line also on real refractivity (even in clear air), and (2) droplets (liquid clouds and rain) and ice crystals (ice clouds) affect real refractivity (scattering).

[28] To quantify this effect, we computed a worst case difference between the real refractivity at 10 and 22.6 GHz (the low and high channels of the ACE+ mission concept), assuming 30 hPa water vapor pressure, 5 g/m³ liquid water content, and a heavy rain rate of 20 mm/h (ice water content can be ignored as generally too small for any appreciable contribution). This results in a real refractivity difference $\Delta N = 0.25$ N units (parts per million), which approximately corresponds to a temperature retrieval error of 0.25 K. Because our method is based on CT technique, where bending angles and absorption are computed as functions of impact parameter, we need to estimate the separation of two rays for the two frequency channels, with the same impact parameter. The ray separation at the perigee point can be estimated as $10^{-6} r_E \Delta N \approx 1.5$ m, where $r_E = 6370$ km is the Earth's radius. Obviously, this effect is very small and will not result in any visible errors in the retrieved differential absorption. Under conditions of a heavy rain, transmission for 10–22.6 GHz frequencies cannot be accurately retrieved for a different reason, because strong absorption will severely degrade the signal-to-noise ratio of the measured signal. Rain effects will typically be relevant below 2–3 km only, however.

[29] In the numerical simulation, we did not model atmospheric particulates, such as clouds and aerosol, that is, the non-clear air atmosphere. While these can significantly affect absorption, this is not expected to be a problem, because the source of the absorption, whether gaseous or particulate, is not essential for the technique introduced, which focuses on mitigating turbulence effects which root in real refractivity only.

[30] One more factor that might degrade the performance of the differential method is the ionosphere. Ionospheric errors can result from the horizontal inhomogeneities in the ionosphere. For a spherically symmetric ionosphere two tropospheric rays with the same impact parameter will have the same perigee point. Horizontal inhomogeneity in the ionosphere will result in additional impact parameter perturbation, which will depend on the frequency. Worst case perturbations of the impact parameter due to the ionosphere in L band (GPS radio occultations) can be estimated as ~ 50 m [Gorbunov et al., 2002]. For the X/K band, the influence of the ionosphere is approximately 100 times smaller. Therefore the ionospheric effect should also

amount to <1 m ray separation in all cases eventually, which is negligibly small.

5. Conclusions and Outlook

[31] Processing X/K band radio occultation data in the presence of turbulence poses a significant challenge because of the scintillations imposed by the turbulence in the measured amplitude profiles. In earlier transmission retrieval approaches, the possibility was discussed of retrieving differential absorption from the direct ratio of measured amplitudes for two different (closely spaced) frequency channels. Here we discussed an advanced differential method of retrieval of atmospheric transmissions based on the ratio of the CT amplitudes.

[32] The new method results in much more accurate correction for turbulence scintillations, as compared to taking the direct ratio of the measured wave fields. This is because of the following reasons: (1) The CT mapping corrects for diffraction and multipath propagation effects. (2) The resulting transformed field is independent from diffraction except for small scales below about 50 m [Gorbunov, 2002b; Gorbunov et al., 2004]. (3) The ratio of the transformed amplitudes then further corrects for small-scale scintillations and effects of the nonsphericity of the atmosphere. (4) The new method does not impose any significant restriction on the frequency difference Δf between the channels, and there is no requirement that Δf be small (e.g., clearly smaller than 1 GHz). This has important technical advantages and provides good differential transmission sensitivity if spacings of a few gigahertz are chosen (e.g., 10 and 17 GHz or 17 and 20 GHz, or similar). The simulations described by Gorbunov and Kirchengast [2005] showed that large frequency separation is more favorable for the method because it results in larger differential transmissions with approximately the same noise level.

[33] We performed numerical simulations with a quasi-realistic model of the turbulent atmospheric refractivity field in a rigorous forward-inverse modeling framework. The model also included receiver noise at a realistic level (carrier-to-noise 67 dBHz, ACE+ mission baseline). These numerical simulations showed the high capabilities of the CT differential method. The influence of the noise is only significant below a ray impact height of 4 km (below 2–3 km altitude), where the signal-to-noise ratio becomes small because of strong absorption and defocusing in the lower troposphere. In this context, the minimum required sampling rate is found to be 1 kHz for adequate wave optics processing of X/K band occultation data. Effects of small amplitude drifts of 0.5% over 20 s (ACE+ mission specification for maximum drift) were also assessed and were found to be of minor relevance compared to thermal noise and of no further concern.

[34] Processing differential transmissions further to imaginary refractivity and, in turn, together with real refractivity derived from bending angles, to atmospheric profiles is a procedure identical to using single-channel transmissions [Kursinski *et al.*, 2002; Kirchengast *et al.*, 2004b, 2004a]. Because of the differencing, there is one differential transmission profile less, however, than single-channel transmission profiles. In the case of ACE+ with three frequencies, this implies availability of two differential transmission profiles, which are still sufficient in combination with the real refractivity profile to separate water vapor and liquid water from temperature, down into the lower troposphere (cf. Gorbunov and Kirchengast [2005] for more details).

[35] Further efforts to perform the explicit turbulence modeling at higher resolution (e.g., down to inner scale of turbulence of 10 m instead of 30 m and down to anisotropy coefficients as small as 5) will be worthwhile, for assessment of the theoretical expectation that residual errors will become smaller when approaching isotropic turbulence, because the scintillation power decreases with the decrease of the anisotropy coefficient [Gurvich, 1984, 1989; Gurvich and Brekhovskikh, 2001]. Another important task will be a theoretical estimation of the effects of diffraction on small-scale inhomogeneities.

[36] Independent of such further work, there is clear evidence from the present study already that in those turbulent cases where single-channel transmissions might be too noisy to be processed directly, the use of differential transmissions is an adequate alternative. It can be expected, on the basis of the experience from single-channel transmission processing [Kirchengast *et al.*, 2004b], that complementary use of the method presented, CT differential transmissions, will make it possible to meet X/K band occultation observation requirements as laid out for ACE+ even better than assessed so far.

[37] **Acknowledgments.** The authors gratefully acknowledge valuable discussions related to this work with A. S. Gurvich (IAPH Moscow, Russia), S. V. Sokolovskiy (UCAR, Boulder, Colorado), F. Cuccoli (University of Florence, Italy), S. Bühler (University of Bremen, Germany), P. Silvestrin (ESA/ESTEC, Noordwijk, Netherlands), and further colleagues of the ESA-ACEPASS study team. The work was funded by ESA under ESTEC contract 16743/02/NL/FF (ESA-ACEPASS study).

References

- Facheris, L., and F. Cuccoli (2003), Analysis of differential spectral attenuation measurements applied to a LEO-LEO link, *ESA-ACEPASS Rep. 16743/02/NL/FF*, Inst. of Electron. and Telecommun., Univ. of Florence, Florence, Italy.
- Fritts, D. C., and M. J. Alexander (2003), Gravity wave dynamics and effects in the middle atmosphere, *Rev. Geophys.*, *41*(1), 1003, doi:10.1029/2001RG000106.
- Fritts, D. C., and T. E. VanZandt (1993), Spectral estimates of gravity wave energy and momentum fluxes. part 1: Energy dissipation, acceleration, and constraints, *J. Atmos. Sci.*, *50*, 3685–3694.
- Fritts, D. C., T. Tsuda, T. Sato, S. Fukao, and S. Kato (1988), Observational evidence of a saturated gravity wave spectrum in the troposphere and lower stratosphere, *J. Atmos. Sci.*, *45*, 1741–1758.
- Gorbunov, M. E. (2002a), Canonical transform method for processing GPS radio occultation data in lower troposphere, *Radio Sci.*, *37*(5), 1076, doi:10.1029/2000RS002592.
- Gorbunov, M. E. (2002b), Radio-holographic analysis of Microlab-1 radio occultation data in the lower troposphere, *J. Geophys. Res.*, *107*(D12), 4156, doi:10.1029/2001JD000889.
- Gorbunov, M. E., and G. Kirchengast (2005), Advanced wave-optics processing of LEO-LEO radio occultation data in presence of turbulence, *ESA/ESTEC Tech. Rep. 1/2005*, Univ. of Graz, Graz, Austria.
- Gorbunov, M. E., and L. Kornbluh (2001), Analysis and validation of GPS/MET radio occultation data, *J. Geophys. Res.*, *106*, 17,161–17,169.
- Gorbunov, M. E., and K. B. Lauritsen (2002), Canonical transform methods for radio occultation data, *Sci. Rep. 02-10*, Dan. Meteorol. Inst., Copenhagen. (Available at <http://www.dmi.dk/dmi/Sr02-10.pdf>.)
- Gorbunov, M. E., and K. B. Lauritsen (2004), Analysis of wave fields by Fourier integral operators and its application for radio occultations, *Radio Sci.*, *39*, RS4010, doi:10.1029/2003RS002971.
- Gorbunov, M. E., A. S. Gurvich, and A. V. Shmakov (2002), Back-propagation and radio-holographic methods for investigation of sporadic ionospheric *E*-layers from Microlab-1 data, *Int. J. Remote Sens.*, *23*, 675–685.
- Gorbunov, M. E., H.-H. Benzon, A. S. Jensen, M. S. Lohmann, and A. S. Nielsen (2004), Comparative analysis of radio occultation processing approaches based on Fourier integral operators, *Radio Sci.*, *39*, RS6004, doi:10.1029/2003RS002916.
- Gurvich, A. S. (1984), Fluctuations during observations of extraterrestrial sources from space through the atmosphere of the Earth, *Radiophys. Quantum Electron.*, *27*, 665–672.
- Gurvich, A. S. (1989), Scintillation spectra during observations of star obscurations by the Earth's atmosphere, *Atmos. Opt.*, *2*, 188–193.
- Gurvich, A. S., and V. L. Brekhovskikh (2001), Study of the turbulence and inner waves in the stratosphere based on the observations of stellar scintillations from space: A model of scintillation spectra, *Waves Random Media*, *11*, 163–181.
- Gurvich, A. S., and I. P. Chunchuzov (2003), Parameters of the fine density structure in the stratosphere obtained from spacecraft observations of stellar scintillations, *J. Geophys. Res.*, *108*(D5), 4166, doi:10.1029/2002JD002281.
- Gurvich, A. S., and I. P. Chunchuzov (2005), Estimates of characteristic scales in the spectrum of internal waves in

- the stratosphere obtained from space observations of stellar scintillations, *J. Geophys. Res.*, *110*, D03114, doi:10.1029/2004JD005199.
- Ishimaru, A. (1978), *Wave Propagation and Scattering in Random Media*, vol. 2, Elsevier, New York.
- Jensen, A. S., M. S. Lohmann, H.-H. Benzon, and A. S. Nielsen (2003), Full spectrum inversion of radio occultation signals, *Radio Sci.*, *38*(3), 1040, doi:10.1029/2002RS002763.
- Jensen, A.S., M. S. Lohmann, A. S. Nielsen, and H.-H. Benzon (2004), Geometrical optics phase matching of radio occultation signals, *Radio Sci.*, *39*, RS3009, doi:10.1029/2003RS002899.
- Kan, V., S. S. Matyugov, and O. I. Yakovlev (2002), The structure of stratospheric irregularities according to radio-occultation data obtained using satellite-to-satellite paths, *Izv. Vyssh. Uchebn. Zaved Radiofiz.*, *45*, 652–663.
- Kirchengast, G., and P. Høeg (2004), The ACE+ mission: Atmosphere and climate explorer based on GNSS-LEO and LEO-LEO radio occultation, in *Occultations for Probing Atmosphere and Climate*, edited by A. K. S. G. Kirchengast and U. Foelsche, pp. 201–220, Springer, New York.
- Kirchengast, G., J. Fritzer, M. Schwaerz, S. Schweitzer, and L. Kornblueh (2004a), The atmosphere and climate explorer mission ACE+: Scientific algorithms and performance overview, *ESA/ESTEC Tech. Rep. 2/2004*, Inst. for Geophys., Astrophys., and Meteorol., Univ. of Graz, Graz, Austria.
- Kirchengast, G., S. Schweitzer, J. Ramsauer, J. Fritzer, and M. Schwaerz (2004b), Atmospheric profiles retrieved from ACE+ LEO-LEO occultation data: Statistical performance analysis using geometric optics processing, *ESA/ESTEC Tech. Rep. 1/2004*, Inst. for Geophys., Astrophys., and Meteorol., Univ. of Graz, Graz, Austria.
- Kursinski, E. R., G. A. Hajj, S. Leroy, and B. Herman (2000), The GPS radio occultation technique, *Terr. Atmos. Oceanic Sci.*, *11*, 53–114.
- Kursinski, E. R., S. Syndergaard, D. Flittner, D. Feng, G. Hajj, B. Herman, D. Ward, and T. Yunck (2002), A microwave occultation observing system optimized to characterize atmospheric water, temperature and geopotential via absorption, *J. Atmos. Oceanic Technol.*, *19*, 1897–1914.
- Lohmann, M. S., A. S. Jensen, H.-H. Benzon, and A. S. Nielsen (2003a), Radio occultation retrieval of atmospheric absorption based on FSI, *Sci. Rep. 03-20*, Dan. Meteorol. Inst., Copenhagen.
- Lohmann, M. S., L. Olsen, H.-H. Benzon, A. S. Nielsen, A. S. Jensen, and P. Høeg (2003b), Water vapour profiling using LEO-LEO inter-satellite links, paper presented at Atmospheric Remote Sensing Using Satellite Navigation Systems, Union Radio Sci. Int., Matera, Italy.
- Rytov, S. M., Y. A. Kravtsov, and V. Tatarskii (1989), *Principles of Statistical Radiophysics: Wave Propagation Through Random Media*, vol. 4, Springer, New York.
- Sokolovskiy, S. V. (2001), Tracking tropospheric radio occultation signals from low Earth orbit, *Radio Sci.*, *36*, 483–498.
- Tatarskii, V. I. (1961), *Wave Propagation in a Turbulent Medium*, MacGraw-Hill, New York.
- Yakovlev, O. I., S. S. Matyugov, and I. A. Vilkov (1995), Attenuation and scintillation of radio waves in the Earth's atmosphere from radio occultation experiment on satellite-to-satellite links, *Radio Sci.*, *30*, 591–602.
- Yakovlev, O. I., S. S. Matyugov, and V. A. Anufriev (2003), Scintillations of centimeter waves and the atmospheric irregularities from radio occultation data, *Radio Sci.*, *38*(2), 1019, doi:10.1029/2000RS002546.

M. E. Gorbunov, Obukhov Institute of Atmospheric Physics, Pyzhevsky per. 3, Moscow 119017, Russia. (gorbunov@dkrz.de)

G. Kirchengast, Institute for Geophysics, Astrophysics, and Meteorology, University of Graz, Universitätsplatz 5, Graz A-8010, Austria.